

Comammox *Nitrospira* bacteria outnumber canonical nitrifiers irrespective of electron donor mode and availability in biofiltration systems

Katherine J. Vilardi¹, Irmarie Cotto¹, Maria Sevillano¹, Zihan Dai^{2,3}, Christopher L. Anderson¹ and Ameet Pinto^{4*}

¹Department of Civil and Environmental Engineering, Northeastern University, Boston, MA 02115, USA

²Key Laboratory of Drinking Water Science and Technology, Research Center for Eco-Environmental Sciences, Chinese Academy of Sciences, Beijing, 100085, China

³University of Chinese Academy of Sciences, Beijing, 100864, China

⁴School of Civil and Environmental Engineering, Georgia Institute of Technology, Atlanta, GA 30332, USA

*Corresponding author: 3226 Ford ES&T, 311 Ferst Drive, Atlanta, GA 30318, USA. Tel: +1 (404) 385-4579; E-mail: ameet.pinto@ce.gatech.edu

One sentence summary: To better understand the comammox bacterial role within these complex nitrifying communities, we investigated their population dynamics across two nitrogen sources (ammonia or urea) at three total nitrogen dosing strategies.

Editor: Tillmann Lueders

Abstract

Complete ammonia oxidizing bacteria coexist with canonical ammonia and nitrite oxidizing bacteria in a wide range of environments. Whether this is due to competitive or cooperative interactions, or a result of niche separation is not yet clear. Understanding the factors driving coexistence of nitrifiers is critical to manage nitrification processes occurring in engineered and natural ecosystems. In this study, microcosm-based experiments were used to investigate the impact of nitrogen source and loading on the population dynamics of nitrifiers in drinking water biofilter media. Shotgun sequencing of DNA followed by co-assembly and reconstruction of metagenome assembled genomes revealed clade A2 comammox bacteria were likely the primary nitrifiers within microcosms and increased in abundance over *Nitrosomonas*-like ammonia and *Nitrospira*-like nitrite oxidizing bacteria irrespective of nitrogen source type or loading. Changes in comammox bacterial abundance did not correlate with either ammonia or nitrite oxidizing bacterial abundance in urea-amended systems, where metabolic reconstruction indicated potential for cross-feeding between strict ammonia and nitrite oxidizers. In contrast, comammox bacterial abundance demonstrated a negative correlation with nitrite oxidizers in ammonia-amended systems. This suggests potentially weaker synergistic relationships between strict ammonia and nitrite oxidizers might enable comammox bacteria to displace strict nitrite oxidizers from complex nitrifying communities.

Keywords: comammox bacteria, drinking water biofiltration, electron donor, nitrification

Introduction

Nitrification, the biological transformation of ammonia to nitrate via nitrite, is an important process in engineered and natural ecosystems. While nitrification mediated by ammonia oxidizing microorganisms (AOM; Kowalchuk and Stephen 2001, Stahl and de la Torre 2012), including ammonia oxidizing bacteria (AOB) and archaea (AOA), and nitrite oxidizing bacteria (NOB; Daims et al. 2016) has been extensively investigated, complete ammonia oxidation (comammox) performed by comammox bacteria is understudied in large part due to its recent discovery. All known comammox bacteria belong to *Nitrospira* sublineage II (Daims et al. 2015, van Kessel et al. 2015, Pinto et al. 2016), and are currently divided into two clades, A and B, with clade A further separated into subclades A1 and A2 (Palomo et al. 2019). Due to close phylogenetic relatedness, comammox-*Nitrospira* cannot be distinguished from *Nitrospira*-NOB based on the 16S rRNA gene sequence or the marker genes for nitrite oxidation (*nxrA* and *nxrB*; Daims et al. 2015). Thus, characterization of comammox bacteria has been largely enabled by shotgun DNA sequencing followed by reconstruction of assembled genomes (Palomo et al. 2016, Pinto et al. 2016, Camejo et al. 2017, Wang et al. 2017, Annavajhala et al. 2018, Poghosyan et al. 2019) and the development of primers targeting subunits of comammox bacterial ammonia monooxygenase (*amo*)

gene (Bartelme et al. 2017, Pjevac et al. 2017, Fowler et al. 2018, Wang et al. 2018, Beach and Noguera 2019, Cotto et al. 2020).

Within the engineered water cycle, clade A1 comammox bacteria have been primarily detected in wastewater treatment plants, while clades A2 and B have been associated with drinking water treatment and distribution systems (Palomo et al. 2019). It is unclear if this translates into physiological differences between the clades/subclades, since there is only one comammox isolate and an enrichment whose kinetic parameters have been reported. To date, kinetic parameters of comammox bacteria are confined to two clade A representatives, cultured *Candidatus Nitrospira inopinata* and an enrichment of *Candidatus Nitrospira kretii* (Kits et al. 2017, Sakoula et al. 2020). Both demonstrate a high affinity for ammonia, with half-saturation constants orders of magnitude lower than strict AOB. Comparatively, the *Candidatus N. kretii* enrichment exhibited a higher affinity for nitrite compared to *Candidatus N. inopinata* and demonstrated partial inhibition of ammonia oxidation even at low ammonia concentrations (Sakoula et al. 2020). Further at the genome-level, the two clades exhibit differences in terms of ammonia transporters, acquisition of alternative ammonia sources (cyanate), and potential use of alternative energy sources (Palomo et al. 2018, Spasov et al. 2020, Yang et al. 2020, Xu et al. 2022). This suggests that clade-specific comammox

Received: November 14, 2021. Revised: February 20, 2022. Accepted: March 21, 2022

© The Author(s) 2022. Published by Oxford University Press on behalf of FEMS. All rights reserved. For permissions, please e-mail: journals.permissions@oup.com

bacterial niche, if applicable, may be arise from any one or combination of several factors. Beyond clade specific traits, identifying the potential environmental and physiological factors driving the coexistence of comammox bacteria with canonical nitrifiers is also important to better understand comammox bacteria role in complex nitrifying communities (Gulay et al. 2019, Liu et al. 2019, Wang et al. 2019a,b, Zheng et al. 2019, Gottshall et al. 2020, Wang et al. 2020, He et al. 2021, Shao and Wu 2021). Comammox bacteria have been detected along with their canonical nitrifying counterparts in wastewater treatment plants (Gonzalez-Martinez et al. 2016, Roots et al. 2019, Zheng et al. 2019, Cotto et al. 2020, Yang et al. 2020), drinking water systems (Pinto et al. 2016, Tatari et al. 2017, Wang et al. 2017, Fowler et al. 2018, Poghosyan et al. 2020), and soils (Prosser and Nicol 2012, Shi et al. 2018, Liu et al. 2019, He et al. 2021) at varying abundances over a wide range of ammonium concentrations. While there is currently no quantitative estimate of the contribution of comammox bacteria to nitrification compared to AOB and NOB, several studies have investigated comammox bacterial dynamics in the context of mixed nitrifying communities. For instance, DNA/RNA stable isotope probing provided support for comammox *Nitrospira* contributing to ammonia oxidation in lab-scale biofilters exposed to very low ammonium concentrations (Gulay et al. 2019). Soil microcosms amended with high ammonia concentrations were enriched in AOB compared to those with lower ammonia concentrations where clade B comammox bacteria proliferated (Wang et al. 2019a, He et al. 2021). Interestingly, in a lab-scale partial nitrification-anammox reactor operating with incrementally increased ammonia loadings, comammox bacteria initially dominated over strict AOB, but its abundance significantly declined as loadings were further increased (Shao and Wu 2021).

Comammox bacteria may also acquire ammonia via urea degradation. Specifically, genes encoding for urea transport and the urease enzyme are distributed among many *Nitrospira* populations (Koch et al. 2015), including most comammox populations (Palomo et al. 2018). While this may diversify potential nitrogen sources for comammox bacteria (Daims et al. 2016), this could be a potential advantage for canonical nitrifiers involved in a reciprocal feeding strategy as observed with co-cultured *Nitrospira moscoviensis* converting urea to ammonia for *N. europaea* (Koch et al. 2015). The tight interplay between canonical nitrifiers is well established; however, our understanding of comammox competition (or lack thereof) with AOM and its impact on strict NOB in mixed communities is limited.

To better understand the comammox bacterial role within these complex nitrifying communities, we investigated their population dynamics across two nitrogen sources (ammonia or urea) at three total nitrogen dosing strategies. Thus, the objectives of this study were (1) to determine if comammox bacteria and canonical nitrifiers exhibit concentration and nitrogen source dependent dynamics when subject to repeat nitrogen amendments and (2) to determine if these dynamics are consistent or variable at the clade or population within each functional guild. Characterization of microbial communities in biofilters at DWTPs has revealed rich nitrifier diversity (Fowler et al. 2018, Gulay et al. 2019), making it an ideal sample source for this study. Collectively, our microcosm-based study offers novel insights regarding the eco-physiology of clade A2-associated comammox bacteria; information on this clade are very limited. Further, while other microcosm studies have focused on competitive interactions between comammox bacteria and strict AOB under controlled conditions (Wang et al. 2019b, He et al. 2021), there is only limited assessment of NOB response to experimental treatment. This study explicitly

assesses the NOB dynamics in response to nitrogen source and loading rates in the context of the broader nitrifying community.

Materials and methods

Experimental design and execution

Granular activated carbon (GAC) with coexisting AOB, NOB, and comammox bacterial populations from biofilters at the drinking water treatment plant (DWTP) in Ann Arbor, (AA) Michigan was used as the inoculum for this experimental work (Pinto et al. 2016). Microcosms consisted of 3 g of GAC supplemented with 10 ml of filter influent from AA DWTP in 40-ml presterilized glass vials (DWK Life Sciences—Fisher 033395C). A total of 96 glass microcosms were prepared such that two biological replicates for each of the three nitrogen concentrations (1.5, 3.5, and 14 mg-N/l) for the two nitrogen sources (i.e. ammonium (direct) and urea (indirect)) were harvested weekly for analyses over the period of the 8-week experiment. Ammonium was spiked in at 0.1, 0.25, and 1 mM (in the form of ammonium chloride solution), corresponding to final concentrations of 1.5, 3.5, and 14 mg-N/l. For urea, 0.05, 0.125, and 0.5 mM (in the form of urea solution) were used to ensure similar concentrations of total nitrogen as the ammonium microcosms. Microcosms were maintained by carefully removing approximately 10 ml of spent filter influent while avoiding the top layer of GAC and subsequently replenishing them with 10 ml of fresh influent and the respective nitrogen source spike every 2 days. The spent filter influent was filtered through 0.2 μ m filters (Sartorius Minisart NML Syringe Filter—Fisher Scientific 14555269) for chemical analyses. The sampled aqueous volume was replaced with fresh substrate to replenish the ammonia and urea concentrations to microcosm specific concentrations. Once a week, two microcosms per condition (i.e. nitrogen concentration and nitrogen source) were sacrificed and two 0.5 g GAC samples from each microcosm were transferred to Lysing Matrix E tubes (MP Biomedical Lysing Matrix E—Fisher MP116914100) and stored at -80°C until further processing. Hach Company Test n' Tube Vials were used to determine concentrations of ammonia-N (Hach, Cat No. 2606945), nitrite-N (Hach, Cat No. 2608345), and nitrate-N (Hach, Cat No. 2605345) in microcosms. All samples were analyzed on a Hach DR1900 photospectrometer (Hach—DR1900-01H). Alkalinity of filtered liquid samples were measured using Hach Alkalinity Total TNTplus Vials (Hach—TNT870).

DNA extraction and qPCR

GAC samples were subjected to DNA extraction using the DNAeasy PowerSoil kit (Qiagen, Inc—Cat No.12888) on the QIAcube (Qiagen, Inc—Cat No. 9002160) following manufacturer's instructions with a few modifications. Specifically, the lysing buffer from the PowerBead tubes were transferred to the Lysing Matrix E tubes and C1 buffer was added. Prior to bead beating, an equal volume of chloroform was added (610 μ l). Bead beating consisted of four rounds of 40 s on a FastPrep-24 instrument (MP Bio—116005500) with bead beading tubes placed on ice for 2 min between each bead beating. Samples were then centrifuged at 10,000 g for 1 min and 750 μ l of aqueous phase used to purify DNA using the QIAcube Protocol for the DNAeasy PowerSoil Kit. Each round of extractions included a reagent blank as a negative control. After extraction, DNA concentration was determined using a Qubit instrument with the dsDNA Broad Range Assay (ThermoFisher Scientific—Cat No. Q32850; Table S1, Supporting Information). DNA was stored in a -80°C freezer until future use.

qPCR assays were conducted using QuantStudio 3 Real-Time PCR System (ThermoFisher Scientific—Cat. No. A28567). Primer sets targeting the 16S rRNA gene of AOB (Hermansson and Lindgren 2001), 16S rRNA gene of Nitrospira (Graham et al. 2007), amoB gene of clade A comammox bacteria (Cotto et al. 2020), and 16S rRNA gene for total bacteria (Caporaso et al. 2011) were used (Table S2, Supporting Information). Previously published primer set for the amoB gene of clade A comammox bacteria was updated based on metagenomic data generated as part of this study (Cotto et al. 2020). Based on alignments of amoB gene sequences from the comammox MAGs assembled in this study, the previously published forward primer for comammox clade A amoB gene from Cotto et al. (2020) had one mismatch with a amoB gene found in metagenome data. Thus, this forward primer was further modified by changing the 13th position from G to a degenerate base S (seven base pairs from 3'-end). The use of the modified primers resulted in increased abundance of comammox bacteria in this study as shown in Figure S1 (Supporting Information), indicating the ability to capture comammox amoB gene sequences not amplified by previous primer set.

The qPCR reactions were carried out in 20 μ l volumes, which included 10 μ l Luna Universal qPCR Master Mix (New England Biolabs, Inc., Cat. No. NC1276266), 5 μ l of 10-fold diluted template DNA, primer concentrations are outlined in Table S2 (Supporting Information) and DNase/RNase free water (Fisher Scientific, Cat. No. 10977015) to make up the remaining volume to 20 μ l. Each sample per assay was subject to qPCR in triplicate and qPCR plates were prepared using the epMotion M5073 liquid handling system (Eppendorf, Cat. No. 5073000205D). The cycling conditions used in this study were as follows: initial denaturing at 95°C for 1 min, 40 cycles of denaturing at 95°C for 15 s, annealing temperatures and time used are listed in Table S2 (Supporting Information) and extension at 72°C for 1 min. qPCR analysis proceeded with a negative control and 7-point standard curve ranging from 10³ to 10⁹ copies of 16S rRNA gene of *N. europaea* for total bacteria quantification, 10²–10⁸ copies of 16S rRNA genes of *N. europaea* and *Ca N. inopinata* for AOB and Nitrospira quantification, respectively, and 10²–10⁸ copies of amoB gene of *Ca N. inopinata* for the quantification of comammox bacteria. PCR efficiencies and R² values from qPCR assays are provided in Table S3 (Supporting Information). The primer used to detect the 16S rRNA gene of Nitrospira would inclusively track both comammox-Nitrospira and Nitrospira-NOB. Thus, Nitrospira-NOB abundance was estimated by subtracting the copy number of comammox bacteria amoB from the copy number of 16S rRNA gene of Nitrospira.

Metagenomic analyses

A subset of samples were selected for metagenomic analysis including DNA extracted from the initial GAC inoculum and samples from weeks 4 and 8 ($n = 13$) for all nitrogen sources and dosing strategies. DNA extracts from duplicate microcosms for each time point were pooled in equal mass proportion before sending DNA templates for sequencing at the Roy J. Carver Biotechnology Center at University of Illinois Urbana-Champaign Sequencing Core. A total of two lanes of Illumina NovaSeq were used to generate paired-end reads ranging from 29 to 68 million per sample (2 \times 150-bp read length; Table S4, Supporting Information). Raw paired-end reads were trimmed and quality filtered with fastp (Chen et al. 2018; Table S4, Supporting Information). Filtered reads were mapped to the UniVec Database (National Center for Biotechnology Information) using BWA (Li and Durbin 2009) to remove potential vector contamination. Subsequent un-

mapped reads were extracted, sorted, and indexed using SAMtools v1.3.1 (Li et al. 2009), then converted back to FASTQ using bedtools v2.19.1 (Quinlan and Hall 2010).

Small subunit rRNA sequence reconstruction from quality filtered short reads was carried out using the Phyloflash v3.4 (Gruber-Vodicka et al. 2020). Briefly, bbmap was used to map short reads against the SILVA 138.1 NR99 database with the default minimum identity of 70% followed by assembly of full-length sequences with Spades (kmers = 99,111, 127) and detection of closest-matching database sequences using usearch global within VSEARCH at a minimum identity of 70%. For read pairs, taxonomic classification was performed by taking the lowest common ancestor using SILVA taxonomy (Pruesse et al. 2007). Assembled sequences from all samples belonging to nitrifying bacteria were clustered at 99% identity using vsearch v2.15.2 (Rognes et al. 2016). Reference Nitrospira and Nitrosomonadaceae 16S rRNA reference sequences were obtained from ARB-SILVA and aligned with assembled sequences using muscle v3.8.1551 (Edgar 2004). Construction of 16S rRNA phylogenetic trees for Nitrospira and Nitrosomonadaceae was performed using IQ-TREE v1.6.12 (Nguyen et al. 2015) with model finder option (Kalyaanamoorthy et al. 2017) selecting TIM3+F+I+G4 and TPM2u+F+I+G4 as models for respective trees.

Quality filtered paired-end reads from all samples were co-assembled with metaSPAdes v3.11.1 (Nurk et al. 2017) with k-mers lengths 21, 33, 55, 77, 99, and 119, and phred off-set of 33. Quality evaluation of the assembled scaffolds was performed using Quast v5.0.2 (Gurevich et al. 2013; Table S5, Supporting Information). Open reading frames (ORF) on scaffolds were predicted using Prodigal v2.6.2 (Hyatt et al. 2010) with the 'meta' flag and functional prediction of resulting protein sequences were determined by similarity searches of the KEGG database (Hiroyuki et al. 1999) using kofamscan (Aramaki et al. 2020). Taxonomic classification of scaffolds harboring nitrogen cycling genes was performed using kaiju v1.7.4 (Menzel et al. 2016) against the NCBI nr database with default parameters. CoverM v0.5.0 (www.github.com/wwood/CoverM) was used to calculate reads per kilobase million (RPKM) of these scaffolds as a metric for estimating relative abundance in each sample.

Scaffolds were binned into clusters and manually refined using Anvi'o (v5.1 and 5.5; Eren et al. 2015) with three binning algorithms including CONCOCT (Alneberg et al. 2014), Metabat2 v2.5 (Kang et al. 2019), and Maxbin2 v2.2.7 (Wu et al. 2016). DAS_tool v1.1.2 (Sieber et al. 2018) was used to merge bins from the three approaches to generate final metagenome assembled genomes (MAGs). Completeness and contamination of the final set was determined using CheckM v1.0.7 (Parks et al. 2015) followed by taxonomic classification using the Genome Taxonomy Database Toolkit v1.2.0 with release 89 v04-RS89 (Chaumeil et al. 2019). CoverM was used to calculate RPKM for each bin. Similar to the annotation of the metagenome, functional prediction of bin ORFs were determined by similarity searches against the KEGG database using kofamscan. The annotation of genes of interest were further confirmed by querying protein sequences against the NCBI-nr database using BLASTP. MAGs were also annotated using Prokka as a secondary annotation method (Seemann 2014). The Up-to-date Bacterial Core Gene pipeline (UBCG; Na et al. 2018) with default parameters was used to extract and align a set of 92 single copy core genes from Nitrospira and Nitrosomonas references genomes (Table S6, Supporting Information) and nitrifier MAGs for phylogenomic tree reconstruction. Maximum likelihood trees were generated based on the nucleotide alignment using IQ-TREE with model finder selecting the GTR+F+R10 and GTR+F+R4

models for *Nitrospira* and *Nitrosomonas* trees, respectively, with 1000 bootstrap iterations. For outgroups, two *Leptospirillum* and three *Nitrosospira* genomes were used for *Nitrospira* and *Nitrosomonas* trees, respectively. Pairwise alignments of comammox *amoA* and *hao* and *Nitrospira nxrA* amino acid sequences were created using muscle. Maximum likelihood trees were inferred by IQ-TREE with model finder selecting LG+G4 for the *amoA* tree and LG+I+G4 for *hao* and *nxrA* trees with 1000 bootstrap iterations for each tree. The *amoA* and *hao* amino acid sequences from *N. europaea* and *Nitrosomonas oligotropha* were used as the outgroup for comammox trees. All trees were visualized using the Interactive Tree of Life (itol; Letunic and Bork 2019). Pairwise comparisons of average nucleotide identity of 38 *Nitrospira* and 15 *Nitrosomonadaceae* genomes (Table S6, Supporting Information) with nitrifier MAGs obtained in this study was determined using FastANI v1.31 (Jain et al. 2018).

Statistical analysis

The relative abundance of each nitrifier population was tested to determine if significant differences existed between concentration or source of electron donor types using ANOVA and Welch t-tests, respectively, with R version 4.0.4. Shapiro–Wilks tests were used to test for normality prior to these statistical tests. Linear regression and correlation analysis were used to examine the relationship between the abundance of nitrifying guilds in each of the nitrogen amendments over time.

Results

Microbial community composition in microcosms and nitrogen biotransformation potential

Microcosms consisting of GAC from drinking water biofilters were subject to intermittent amendments of nitrogen using two nitrogen sources (ammonia or urea) across three nitrogen concentrations (14, 3.5, and 1.5 mg-N/l). The conditions used in these experiments are denoted as 14A, 3.5A, 1.5A, 14U, 3.5U, and 1.5U, where A or U represents ammonia or urea amendments, respectively, and the number represents the concentration of nitrogen source spike in mg/l as nitrogen. A total of two microcosms were sacrificed on a weekly basis over the duration of a 8-week experiment ($n = 96$ total microcosms). Extracted DNA from the inocula and weeks 4 and 8 were subject to shotgun DNA sequencing ($n = 13$).

Initial assessment of taxonomic diversity in the samples based on analyses of metagenomic reads mapping to the small subunit rRNA database (SILVA SSU NR99 version 138.1) indicated that the GAC inocula largely consisted of bacteria with archaea and eukaryota constituting a small proportion of the overall metagenomic reads (~0.002%). The bacterial community was primarily composed of Gammaproteobacteria (20%–30%), Alphaproteobacteria (25%–31%), and Nitrospirota (8%–15%; Fig. 1A). *Nitrospira* and *Nitrosomonadaceae* were the only nitrifiers identified and constituted 9%–15% of the overall microbial community in samples. Full length 16S rRNA gene sequences were assembled from each sample ($n = 13$) resulting in a total of eight sequences with closest matching SILVA database hits to uncultured *Nitrospira* bacteria (Accession numbers: MF040566, AY328760, and JN868922). Clustering of all eight *Nitrospira* 16S rRNA gene sequences at 99% identity resulted in two *Nitrospira* operational taxonomic units (OTUs), with one cluster composed of six sequences (*Nitrospira* OTU 1) and the other cluster with two sequences (*Nitrospira* OTU 2). Phylogenetic placements of these OTUs revealed both clus-

tered within *Nitrospira* sublineage II (Figure S2A, Supporting Information). Diversity of *Nitrospira* was likely underrepresented as full length *Nitrospira* 16S rRNA gene sequences could not be assembled from some samples despite a large portion of extracted 16S rRNA gene reads mapping to *Nitrospira* references in the SILVA database. Limited assembly of these reads could be due to several closely related *Nitrospira* species/strains coexisting in the samples making reconstruction of full length sequences difficult. For canonical AOB, *Nitrosomonas* sp. AL212 (CP002552) was the closest matching database hit to one assembled sequence while another six had hits closest to *Nitrosomonadaceae* (Accession numbers: FPLP01009519, KJ807851, and FPLK01002446), but could not be further classified at the genus or species level. Phylogenetic placement of the single *Nitrosomonas* OTU affiliated it with *Nitrosomonas* sp. AL212 and *Nitrosomonas ureae* (Figure S2B, Supporting Information).

Following co-assembly of metagenomic reads, predicted protein coding genes from scaffolds associated with the nitrogen metabolism were taxonomically classified (Fig. 1B). The majority of methane/ammonia monooxygenase (*pmo*–*amo*) like genes (KEGG orthology: K10944, K10945, and K10946) were associated with either nitrifiers (i.e. *Nitrospira* or *Nitrosomonas*) or methanotrophs (i.e. *Methylocystis*; Fig. 1C). While some *amoCAB* genes could not be classified to the genus level using kaiju software, blastp searches against the NCBI nonredundant protein database indicated these were closely related to *Nitrosomonas*. All retrieved *hao* sequences (KEGG orthology: K10535) were associated with *Nitrospira*, which is likely due to the low relative abundance of *Nitrosomonas*-like populations and the resulting inability to assemble their *hao* genes. Potential for ureolytic activity was detected across four phyla based on the urease alpha subunit (*ureC*). *ureC* sequences associated with *Nitrospirota* and *Gammaproteobacteria* could be classified at the genus level as *Nitrospira* and *Nitrosomonas*, respectively. Sequences identified as nitrate reductase/nitrite oxidoreductase alpha and beta subunits (K00370 and K00371) were subject to further classification to differentiate between nitrite oxidoreductase genes belonging to NOB from nitrate reductases belonging to other community members. Phylogenetic placement of most *Nitrospira nxrA* sequences found in this study cluster within a branch containing both comammox and *Nitrospira*-NOB species (*Candidatus N. inopinata*, *Candidatus N. nitrosa*, and *N. defluvii*; Fig. 1D). While other sequences clustered on a separate branch with *Candidatus N. nitrificans*, a single *Nitrospira nxrA* sequence clustered closely within a branch containing only *Nitrospira*-NOB belonging to sublineage II.

Phylogenomic placement of nitrifying populations and their metabolism

MAGs were obtained from GAC microcosms after dereplication from three binning approaches. All 204 MAGs were classified as bacteria, with 145 MAGs exhibiting completeness greater than 70% and contamination less than 10% (Table S7, Supporting Information). Approximately, 62% of the metagenomic reads mapped to these MAGs. A total of nine MAGs were classified as nitrifying bacteria belonging to *Nitrosomonas* and *Nitrospira* (Table S8, Supporting Information). Genome annotation confirmed that four *Nitrospira* MAGs had key ammonia (ammonia monooxygenase and hydroxylamine oxidoreductase) and nitrite (nitrite oxidoreductase) oxidation genes (Figure S3, Supporting Information). Quality assessment for these comammox MAGs indicated two high (Bin_49_2_2 and Bin_49_4) and one medium quality (Bin_260; Table S8, Supporting Information) according to Bowers et al. (2017). A

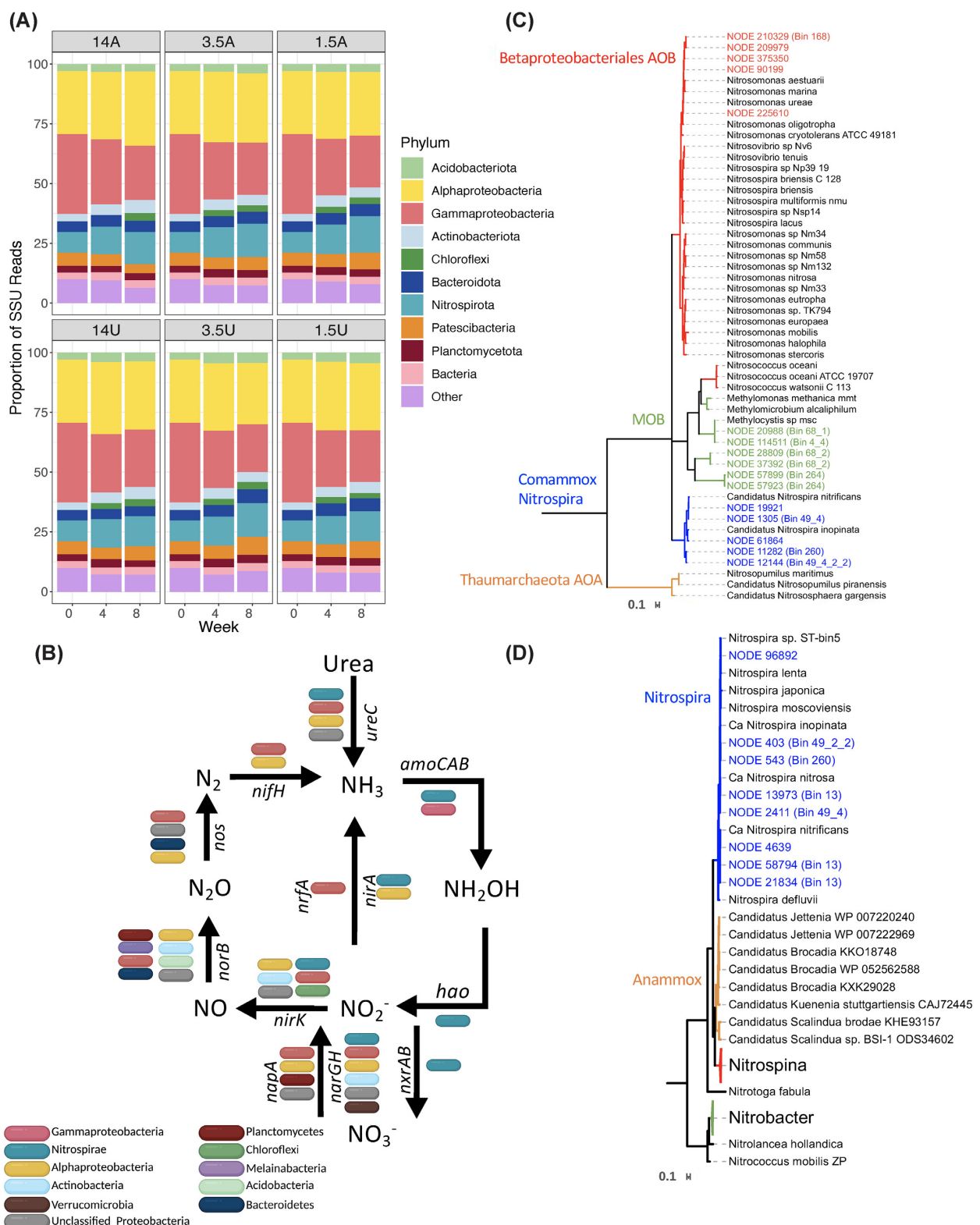


Figure 1. **(A)** Proportion of metagenomic reads mapping to the SILVA SSU NR99 database (version 138.1) from the inocula and treated samples at weeks 4 and 8. The community primarily consisted of Gammaproteobacteria, Alphaproteobacteria, and Nitrospirota. Proteobacteria is broken down by classes, Alphaproteobacteria and Gammaproteobacteria, though a small portion of Proteobacteria reads could not be classified further. **(B)** Taxonomic classification of genes for nitrogen biotransformation present in the metagenome at the phyla level with Proteobacteria presented by classes, Alphaproteobacteria and Gammaproteobacteria. **(C)** and **(D)** Phylogenetic placement of amoA-pmoA like sequences (C), and nxrA sequences (D) detected in the metagenomes. Both maximum likelihood trees were constructed based alignments of protein sequences of the respective genes. Sequences identified in this study are colored according to their phylogenetic placement (red, green, blue, and orange) while references are black. AOB = ammonia oxidizing bacteria and MOB = methane oxidizing bacteria.

fourth comammox MAG (Bin_13) was assembled with high completeness (89%), but also possessed high redundancy (18%) that could not be improved with further manual refinement. The remaining two *Nitrospira* MAGs (Bin_7_1 and Bin_188), which were likely strict NOB due to lack of ammonia oxidation genes, were less complete (38.04% and 48.25%) with low redundancy (8.76% and 8.46%). The low completeness was likely not due to their lower abundance, but potentially high level of strain heterogeneity, which may have affected the assembly of reads associated with *Nitrospira*-NOB. For example, RPKM-based relative abundance estimated using all reads (total RPKM) showed the two *Nitrospira*-NOB MAGs exhibited similar relative abundance to comammox bacteria MAGs Bin_49_2_2 and Bin_49_4 (~7–10 total RPKM), but the CheckM estimated strain heterogeneities for Bin_7_1 and Bin_188 were 40 and 75, respectively, compared to 0 for both Bin_49_2_2 and Bin_49_4. In total, two MAGs classifying as *Nitrosomonas* were deemed high (Bin_83) and medium quality (Bin_168); however, a third *Nitrosomonas* MAG was considered low quality.

A maximum likelihood tree based on 91 single copy core genes confirmed all *Nitrospira* MAGs affiliated with sublineage II (Fig. 2A). A total of four of the *Nitrospira* MAGs from this study clustered within clade A comammox *Nitrospira* (Bin_49_2_2, Bin_49_4, Bin_260, and Bin_13), but were separated into distinct groups on the phylogenomic tree; namely, forming three clusters with MAGs obtained from tap water, drinking water filters, and freshwater. *amoA*-based phylogenetic analysis corroborated their placement into clade A (Fig. 2B); however, *hao*-based phylogeny distinguished three of comammox MAGs (Bin_49_2_2, Bin_49_4, and Bin_260) as clade A2 (Palomo et al. 2019), while one clustered within clade A1 (Bin_13; Fig. 2C). Consistent across all trees, Bin_49_2_2 and Bin_260 cluster closely with comammox MAGs *Nitrospira* sp. SG-bin2 and ST-bin4 (ANI ~ 92%) derived from tap water metagenomes (Wang et al. 2017). Bin_49_4 clustered closely with *Nitrospirae* bacterium Ga0074138 (ANI ~ 99%), which was previously detected in GAC from the same DWTP (Pinto et al. 2016), along with other tap water and groundwater-fed rapid sand filter MAGs (Palomo et al. 2016, Wang et al. 2017). Bin_13 associated with comammox MAGs obtained from freshwater, UBA5698, and UBA5702 (Parks et al. 2017; ANI ~ 90%); however, its high contamination (18%) likely renders ANI comparison less accurate. Overall, the MAGs demonstrated less than 95% ANI to other reference comammox bacterial MAGs (Figure S4, Supporting Information) suggesting comammox bacteria detected in GAC microcosms are distinct from one another and previously published comammox MAGs; as a result, they are likely novel *Nitrospira* species. The two remaining *Nitrospira* MAGs, Bin_7_1 and Bin_188, clustered with strict *Nitrospira*-NOB MAGs recovered from tap water, *Nitrospira* sp. ST-bin5 (Wang et al. 2017; ANI ~ 94%), and a rapid sand filter, *Nitrospira* CG24D (ANI ~ 87%; Palomo et al. 2016; Fig. 2A and Figure S4, Supporting Information). However, since Bin_7_1 and Bin_188 were highly incomplete, the possibly they are novel comammox bacteria cannot be excluded. Only two strict AOB MAGs (Bin_83 and Bin_168) from this study were used for phylogenomic analysis due high redundancy and low completeness of the third (Bin_195). Both Bin_83 and Bin_168 originate from *Nitrosomonas* cluster 6a and clustered closely with *Nitrosomonas ureae* and *Nitrosomonas* sp. AL212 (Fig. 2D). Bin_168 shares a high sequence similarity to *N. ureae* (ANI ~ 98%), while Bin_83 shares less than 83% ANI to any of the references on the tree including Bin_168.

All comammox MAGs demonstrated the potential for ureolytic activity with the presence of the *ureABC* operon in addition to most genes for urease accessory proteins (Figure S2, Supporting

Information). *Nitrospira*-NOB MAGs did not contain genes encoding for urease; however, two *ureC* sequences found on assembled scaffolds that were classified as *Nitrospira* but were not binned into any of the *Nitrospira* MAGs. Queries of these *ureC* genes against the NCBI nonredundant database revealed one sequence shared the highest % identity to *Nitrospira lenta* and *N. moscoviensis*, while top hits for the second sequence belonged to an unclassified *Nitrospira*. In total, one *Nitrospira*-NOB MAG (Bin_7_1) did harbor genes for the urea transport system permease proteins (*urtBC*), urea transport system substrate-binding proteins (*urtA*), and urea transport system ATP-binding proteins (*urtDE*). This suggests that the two unbinned *ureC* genes likely belonged to *Nitrospira*-like NOB bacteria. *Nitrosomonas* MAGs Bin_168 and Bin_83 each contained the *ureCAB* operon and some genes for urease accessory proteins and urea transport. A third *ureC* sequence found in the metagenome classified as *Nitrosomonas* but was not binned into any *Nitrosomonas* MAGs.

The impact of nitrogen amendments on nitrifying populations

To address concentration and nitrogen source-dependent dynamics of the three nitrifier populations detected in our metagenomic analysis, qPCR-assays were used to estimate their abundances over time in the nitrogen-amended microcosms. In the high ammonia amendment (14A), strict AOB relative abundance increased 2.4-fold from weeks 1 to 3 but remained below 2% of total bacteria for the duration of the experiment, whereas comammox relative abundance increased markedly over time reaching 2.8% of total bacteria by end of the experiment (Fig. 3B). Similar to strict AOB, *Nitrospira*-NOB relative abundance increased early on, but thereafter, reduced from 4% at its peak in week 2 to 1.8% by week 8. Weekly measurements for nitrogen concentrations taken alongside biomass samples indicated the presence of residual ammonia and accumulated nitrite concentrations were highest during the first 3 weeks of the experiment, but gradually reduced over time with most inorganic nitrogen present as nitrate (Figure S5, Supporting Information). While comammox bacteria were always dominant, qPCR-based abundance of strict AOB as a portion of AOM was significantly higher when ammonia and nitrite accumulated in weeks 1–3 as compared to weeks 5–8 (Welch's t-test, P-value < .05; Fig. 3A).

The qPCR data was in concordance with metagenomic estimation of MAG abundance with clade A2 comammox (Bin_49_2_2, Bin_49_4, and Bin_260) highly abundant compared to strict AOB (Bin_83, Bin_168, and Bin_195) and clade A1 comammox (Bin_13) in the inocula and at weeks 4 and 8 in the high ammonia amendment (Fig. 4). In particular, clade A2 MAGs Bin_49_2_2 and Bin_49_4 were the most dominant comammox populations, while strict AOB was dominated by Bin_83 at each time point. *Nitrospira*-NOB MAGs had comparable abundance to clade A2 comammox MAGs but displayed limited variation in abundance in the high ammonia amendments. This contrasts with the qPCR data, where *Nitrospira*-NOB were significantly more abundant than comammox bacteria at earlier timepoints and then demonstrated a significant decrease in abundance over time. This is likely due to the fact that the two assembled *Nitrospira*-NOB MAGs do not represent the entirety of NOB diversity in the microcosms as several *nxr* genes were not binned into MAGs and that metagenomic data is only available for select timepoints as compared to qPCR data.

Nitrifier populations in mid and low ammonia amendments displayed similar dynamics to those observed in high ammonia with comammox relative abundance increasing to 3% and 2.2%

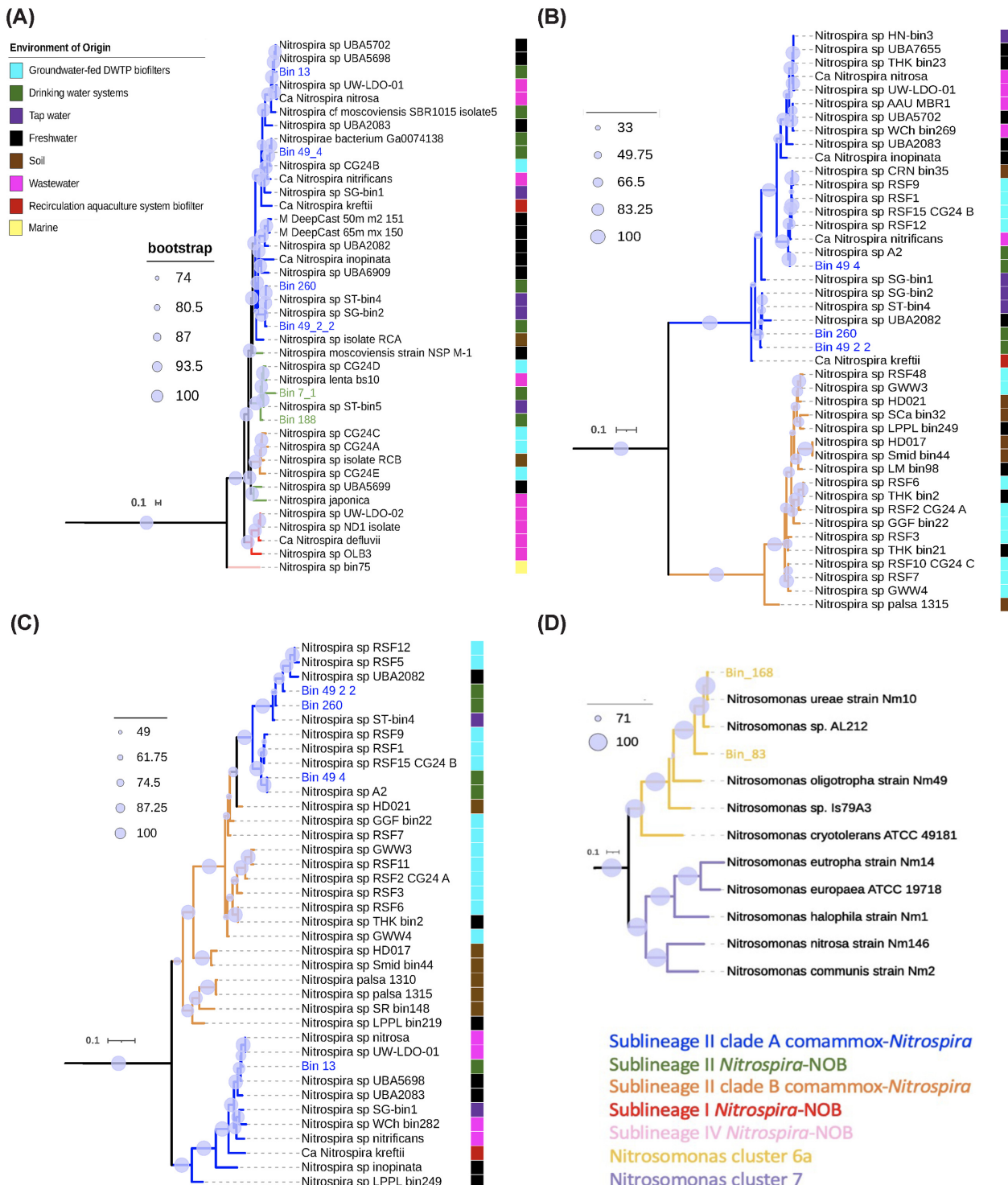


Figure 2. Phylogenomic tree for *Nitrospira* MAGs (blue and green) obtained in this study and 34 reference genomes (black). **(A)** Blue label = comammox, green label = NOB. Branch colors represent different *Nitrospira* sublineages. Two *Leptospirillum* reference genomes were used as the outgroup for maximum likelihood tree construction. **(B)** Maximum likelihood tree based on ammonia monooxygenase subunit A (amoA) sequences from comammox-*Nitrospira*. **(C)** Maximum likelihood tree based on hydroxylamine oxidoreductase (hao) sequences of comammox-*Nitrospira*. For (B) and (C), blue labels represent amoA/hao gene sequences found in comammox MAGs from this study, while black labels are reference sequences. Environment of origin is denoted with colored squares to the left of each tree. amoA and hao protein sequences from *N. europaea* and *N. oligotropha* were used as the outgroup for comammox trees in (B) and (C), respectively. **(D)** Phylogenomic tree for strict AOB MAGs (yellow) obtained in this study and 10 *Nitrosomonas* reference genomes (black). Three *Nitrosospira* genomes were used as the outgroup.

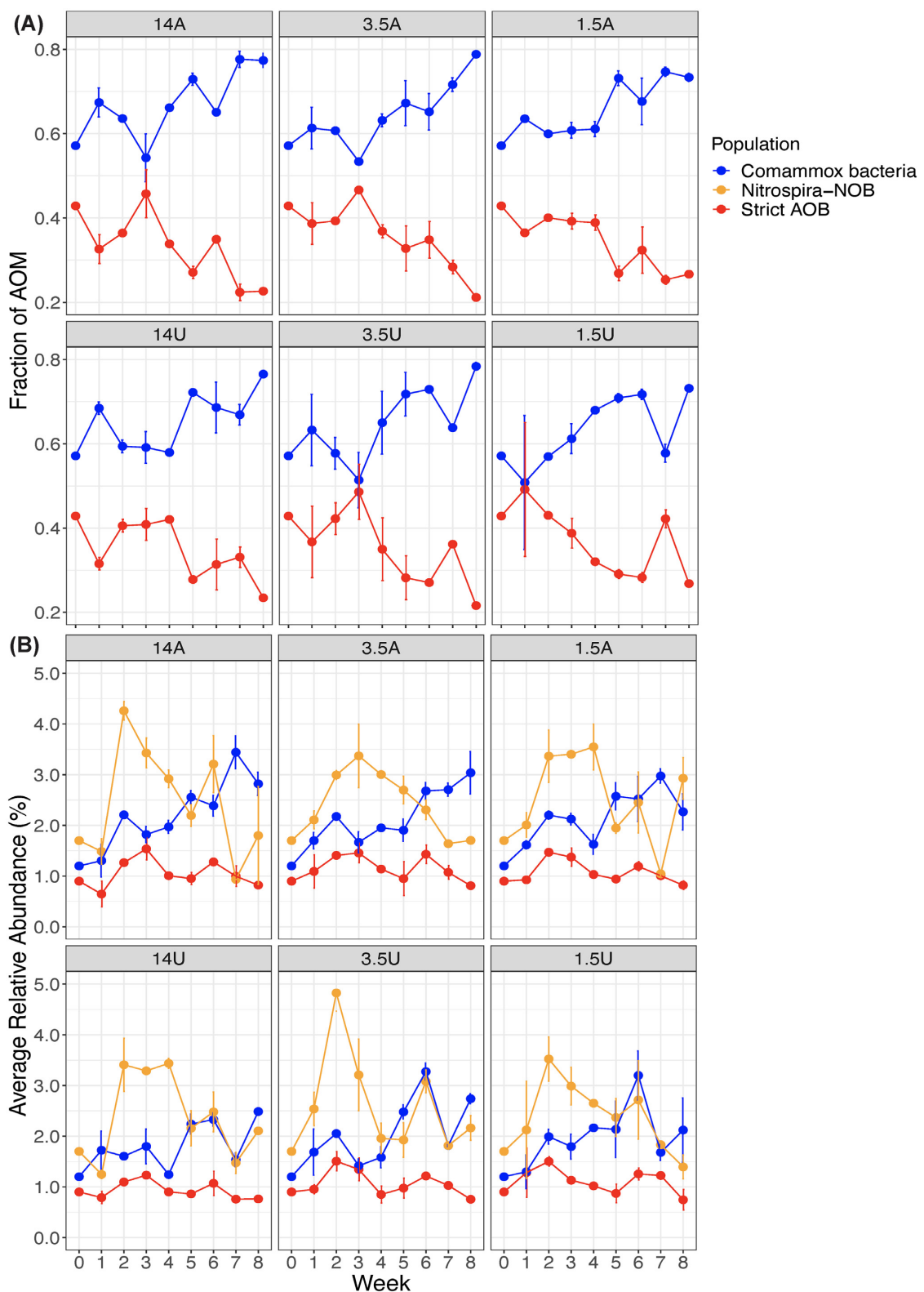


Figure 3. (A) The relative abundance of comammox bacteria (blue) and strict AOB (red) as a proportion of all AOMs calculated using copy number of 16S rRNA and amoB genes of strict AOB and comammox bacteria, respectively and dividing by the combined copy number to represent total AOM for each time point. Data points averaged from triplicate qPCR analyses of samples across biological duplicate microcosms. (B) Relative abundance of comammox bacteria (blue), Nitrospira-NOB (orange), and strict AOB (red) as a proportion of total bacteria using the ratio of copy number of the respective nitrifier genes to copy number of total bacteria averaged between duplicate samples. Panels display relative abundances of the nitrifiers subject to varying nitrogen amendments, where data points represent the average of biological replicates (qPCR performed in triplicate) and error bars for standard deviation.



Figure 4. RPKM calculated for all MAGs identifying as comammox bacteria (blue), Nitrospira-NOB (orange) and strict AOB (red) at selected time points.

of total bacteria by week 8, respectively. Interestingly, Bin_260, the least abundant clade A2 comammox MAG in the inocula, demonstrated significant increase in abundance in the low ammonia amendment over the course of the experiment compared to its abundance in the other ammonia amendments. Consistent with the ammonia-amended microcosms, strict AOB in urea-amended microcosms increased in relative abundance only at earlier time points followed by low but stable relative abundance (~2% of total bacteria). In the high urea amendment, relative abundance of comammox bacteria remained largely unchanged at earlier time points followed by an increase in abundance. Despite this, mean relative abundance of comammox bacteria compared to strict AOB was still approximately 2-fold greater in all urea amendments. Similar to the ammonia amendments, Nitrospira-NOB relative abundance did increase initially followed by a decline in all urea amendments. Interestingly though, the relative abundance of comammox bacteria and Nitrospira-NOB were similar in the later weeks of the experiment after Nitrospira-NOB's initial rise in urea amendments. Clade A2 comammox MAG Bin_260 was consistently lower in abundance than Bin_49_2_2 and Bin_49_2 in the urea amendments except for mid urea. Abundance of the clade A1 comammox MAG remained lower than all clade A2 MAGs and displayed minimal enrichment in all the urea amendments, which was consistent with ammonia-amended microcosms. Bin_168, which showed high sequence similarity to *Nitrosomonas ureae*, did

not exhibit enrichment in any of the urea amendments and remained low in abundance with all other strict AOB MAGs.

There was no significant difference in the mean qPCR-based relative abundance of strict AOB or Nitrospira-NOB between the high ammonia (14A) and urea amendments (14U; Welch t-test, $P > .05$), but the mean relative abundance of comammox bacteria was significantly greater in high ammonia than in the high urea amendment (Welch t-test, $P < .05$). Comparatively, out of all nitrogen amendments, mean relative abundance of comammox bacteria was the lowest in high urea (1.8% of total bacteria). Comparisons between the mid ammonia (3.5A) and urea amendments (3.5U) as well as the low ammonia (1.5A) and urea (1.5U) amendments revealed no significant difference in mean relative abundance for any of the nitrifier populations (Welch t-test, $P > .05$). Additionally, no significant differences were detected when testing the mean relative abundance of the three nitrifier populations between high, mid, and low concentrations within each amendment type (ANOVA, $P > .05$).

The relative abundance of the nitrifying groups were used to examine potential correlations between the different populations in each of the nitrogen amendments. The ratio of AOM to comammox bacteria as a portion of total Nitrospira revealed a strong positive relationship in all amendments (Pearson $R = 0.75$ – 0.87 , $P < .001$) (Figure S6A, Supporting Information), however, the change in relative abundance

of comammox bacteria was not directly correlated with that of strict AOB in any of the nitrogen amendments (Figure S6B, Supporting Information). Strict AOB and *Nitrospira*-NOB abundances were strongly correlated for all urea amendments and high (14A) and mid ammonia (3.5A) (Pearson $r = 0.58$ – 0.82 , $P < .05$, Fig. 5A), but exhibited a weaker relationship in low ammonia (Pearson $r = 0.42$, $P > .05$). Interestingly, while comammox bacteria abundance was significantly and negatively correlated with that of *Nitrospira*-NOB in ammonia amendments (Pearson $r = -0.37$ to -0.61 ; $P < .05$), there was no significant association between them in the urea amendments ($P > .05$; Fig. 5B).

Discussion

Key nitrifiers encompassing *Nitrospira* and *Nitrosomonas*-like bacteria share ureolytic potential.

16S rRNA gene sequences assembled from short reads indicated *Nitrospira* and *Nitrosomonas*-like populations were the only nitrifiers present in the microcosms. The proportion of 16S rRNA gene reads mapping to *Nitrospira*-like populations in this study suggested that they were highly abundant in the inocula and nitrogen amendments. Surveys of other DWTP biofilters using 16S rRNA gene amplicon sequencing have indicated that sublineage II *Nitrospira* account for a dominant portion of the bacterial community (Gulay et al. 2016) with further investigation confirming high contributions to its abundance were from comammox-*Nitrospira* (Palomo et al. 2016, Tatari et al. 2017). The strict AOB OTU found in this study was affiliated with oligotrophic *Nitrosomonas* cluster 6a, which exhibit maximum growth rates at ammonia concentrations similar to the ones used for high and mid nitrogen amendments (Bollmann et al. 2011, Sedlacek et al. 2019). Despite this, the proportions of SSU rRNA gene reads mapping to *Nitrosomonas*-like populations in all nitrogen amendments were consistently low. Taxonomic classification of nitrogen cycling genes revealed metabolic potential for nitrification processes were confined to *Nitrospira* and *Nitrosomonas*-like populations corroborating with assembled 16S rRNA gene sequences. Additionally, phylogeny of *amoA* sequences found in the metagenome indicated ammonia oxidation could be mediated by both *Nitrospira* and *Nitrosomonas*.

We assembled a total of nine nitrifier MAGs which included comammox-*Nitrospira* ($n = 4$), *Nitrospira*-NOB-like ($n = 2$), and *Nitrosomonas*-like ($n = 3$) populations. In total, three of the four comammox MAGs assembled were identified as clade A2 based on phylogenetic analyses of hydroxylamine dehydrogenase (*hao*), which has previously been shown to dominate drinking water biofilters along with comammox clade B (Palomo et al. 2019). The remaining comammox MAG assembled from biofilter media in this study was affiliated with clade A1 based on *hao* gene phylogeny, which while atypical for drinking water biofilters is consistent with previously published metagenome from the AA drinking water filters (Pinto et al. 2016). Similar coexistence of clade A1 and A2 comammox bacteria with canonical nitrifiers has been observed in tertiary rotating biological contactors treating municipal wastewater with low ammonium concentrations (Spasov et al. 2020). However, phylogenomic placement of clade A subgroups in this study separated the comammox MAGs into distinct clusters associated with freshwater (Bin_13, clade A1), groundwater biofilters (Bin_49_4, clade A2), and tap water (Bin_260 and Bin_49_2_2, clade A2). Maintenance of high functional redundancy for the complete ammonia oxidation pathway may rely on coexisting comammox populations avoiding direct competition through dis-

tinct physiological niches. Additionally, the inocula were sourced from low substrate conditions, which may also allow for the coexistence of multiple comammox populations. Strict AOB MAGs obtained in this study associated with low ammonia adapted *Nitrosomonas* cluster 6a (Koops et al. 2006), which is consistent with the inocula source being an oligotrophic environment (i.e. DWTPs). Furthermore, close relatives of *Nitrospira*-NOB MAGs obtained in this study originated from a tap water source where *Nitrospira*-NOB also coexisted with strict AOB and comammox bacteria under oligotrophic conditions (Wang et al. 2017). Our findings, consistent with previous studies, confirm the nitrifier community encompassed multiple populations capable of single and two-step nitrification within a single system with *Nitrospira* as the dominant nitrifier. However, the mechanism behind high abundances of *Nitrospira*-NOB in biofilters is not yet completely understood. One possibility could be that *Nitrospira*-NOB have other roles in these environments besides nitrite oxidation, as their broad metabolic flexibility includes acquiring ammonia from cyanate or urea, aerobic growth on formate and hydrogen, and oxidation of atmospheric hydrogen (Koch et al. 2014, 2015, Palatinszky et al. 2015, Leung et al. 2021). Further, assessment of metabolic versatility revealed initiation of nitrification through urea degradation was possible by all three nitrifying guilds. Though ureolytic activity is a widespread trait among cultured comammox-*Nitrospira* representatives and curated MAGs, the capability is confined to only some *Nitrospira*-NOB and *Nitrosomonas* species (Koch et al. 2015, Sedlacek et al. 2019). Here in particular, this would allow *Nitrospira*-NOB to play a role in nitrite production in urea microcosms by crossing feeding ammonia from urea degradation to strict AOB, a mutualistic strategy, which may not be active in ammonia-amended microcosms.

Comammox bacterial abundance increased irrespective of nitrogen source or loading but may compete with NOB depending on nitrogen source type

We tested the impact of nitrogen source and loading rates on temporal dynamics of a mixed nitrifying community to determine whether comammox bacteria are outcompeted at higher concentrations and/or favored in urea amendments due to their ureolytic activity. qPCR-based abundance tracking revealed comammox bacteria demonstrated a preferential enrichment over strict AOB in the nitrogen amendments irrespective of nitrogen source or availability. Additionally, strict AOB abundance did not exhibit any significant difference across the nitrogen amendment types. This is in contrast to previous work in soil microcosms, where AOB abundance increased in response to high ammonia amendments (He et al. 2021). However, strict AOB populations in these soil microcosms were primarily *Nitrospira* compared to oligotrophic *Nitrosomonas* cluster 6a, which were the primary AOB in this study. Here, both comammox bacteria and strict AOB demonstrated increased abundance in all amendments during the earlier weeks of the experiment. Ultimately, while comammox bacteria were enriched over time our findings demonstrated this increased abundance was not associated with a decrease in the abundance of strict AOB in any of the nitrogen amendments. This suggests a lack of direct competition between the two comammox and strict AOB, which could be attributable to the two ammonia oxidizers occupying separate nitrogen availability niches (Martens-Habbena et al. 2009, Kits et al. 2017). Stable abundances of strict AOB compared to enrichment of comammox could be due to a combination of factors ranging from (1) higher abundances of comammox

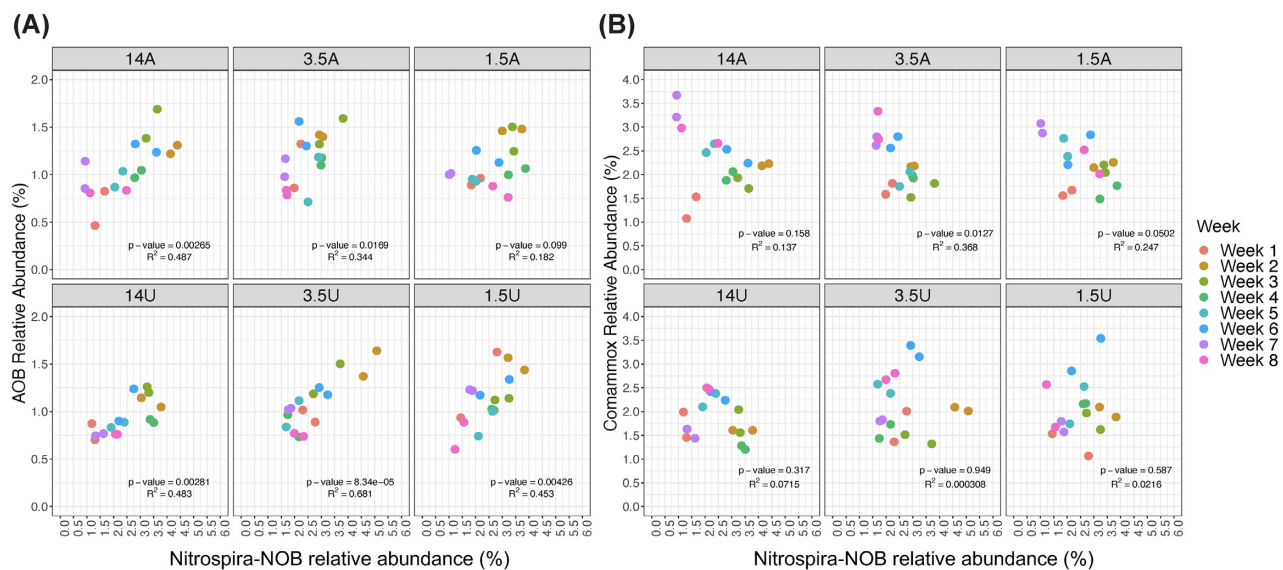


Figure 5. (A) Significant positive correlation between changes in AOB concentration and that of Nitrospira-NOB as a proportion of total bacteria were found in most treatments, except low ammonia (1.5A). **(B)** Negative associations between changes in comammox bacteria concentration and that of Nitrospira-NOB as a proportion of total bacteria existed in ammonia amendments with statistically significance detected in 3.5A and 1.5A, while no association existed in urea amendments.

bacteria in the inocula and (2) significantly higher biomass yields per mole of ammonia oxidizers for comammox bacteria compared to AOB (Kits et al. 2017). While the trends seen suggest increased comammox bacteria abundance does not accompany a decrease in strict AOB abundance in any of the amendments, a longer experimental period would have been ideal considering the slow growth dynamics of nitrifying bacteria.

Clade A2 associated comammox bacterial MAGs were dominant in the inocula and over the course of the experiment showed increased abundance in all amendments. In contrast, comammox bacteria belonging to clade A1 were lower in abundance and did not demonstrate significant change over time in any amended microcosm. Though physiological differences between comammox bacteria clades/subclades have yet to be established, earlier studies of DWTP biofilters have observed higher abundances of clade B (Fowler et al. 2018) or alternatively both clades found at the same DWTP but within separate rapid sand filters, where clade B was more abundant in the secondary filters receiving lower ammonia concentrations (Poghosyan et al. 2020). In this study, the lack of clade A1 enrichment over the course of the experiment may also indicate distinct physiological niches within clades (i.e. subclade-level niche differentiation). Future research is necessary to develop a clearer understanding of physiological differences between comammox bacteria at the clade/subclade level. Since cultivability of comammox bacteria remains an ongoing challenge, integrating multiple 'omics' techniques (i.e. metatranscriptomics and metaproteomics) may be an appropriate strategy for examining ammonia utilization and the expressed metabolisms of multiple coexisting comammox bacteria populations alongside canonical nitrifiers.

The negative association between comammox bacteria and canonical NOB observed in ammonia amendments could be a result of nitrite limitation resulting from complete nitrification driven by comammox bacteria. The possibility of comammox bacteria being a source of leaked nitrite to Nitrospira-NOB seems unlikely in this case as this would likely form a positive association between the two. Nitrite limitation driven competition between comammox bacteria and NOB is supported by the fact the nega-

tive associations between the groups were stronger at medium (3.5 mg-N/l) and low (1.5 mg-N/l) nitrogen availability as compared to the high ammonia amendments (i.e. 14 mg-N/l). In contrast, there was no significant association between the abundance of comammox bacteria and Nitrospira-NOB in the urea-amended systems irrespective of nitrogen loading. We hypothesize that variable observations between ammonia and urea-amended systems likely emerge from the extent of metabolic coupling between AOB and NOB and the resultant ability of comammox to outcompete NOB. Specifically, while the rate of nitrite availability for NOB in ammonia-amended systems is largely dictated by ammonia oxidation activity of AOB, it is likely that nitrite availability in urea-amended systems would be dictated by a combination of both AOB activity and indirectly by NOB. In this case, the production of nitrite could be mediated by Nitrospira-NOB capable of ureolytic activity by cross-feeding ammonia to strict AOB, who in turn provide nitrite at a rate at which Nitrospira-NOB can metabolize it. This tight coupling between AOB and NOB is supported by stronger and more significant correlation between AOB and NOB abundance in urea-amended systems as compared to ammonia-amended systems. Thus, it appears that while comammox bacteria may outcompete Nitrospira-NOB in systems where AOB abundances are low and nitrite availability is largely dictated by AOB activity, this competitive exclusion may be limited in scenarios with established AOB-NOB cross-feeding via urea where nitrite availability is governed not only by AOB's ammonia oxidation rate but also by NOB's ureolytic activity. Since urea is used directly by urease-positive nitrifiers, variabilities in their affinities for the substrate would play a role in the outcome of competition in urea microcosms, but was not assessed in this study. In contrast to the ammonia-amended systems, comammox bacterial abundance in urea-amended systems exhibited longer acclimation period as compared to the strict AOB; a proportion of the AOB population demonstrated the potential for ureolytic activity. The longer acclimation period for comammox bacteria could be a result of higher metabolic costs of ammonia to nitrite oxidation in comammox bacteria as compared to AOB. This could also be due to the less efficient ammonia transport postureolytic activity in

comammox bacteria that have low affinity ammonia transporters, and thus ammonia availability could be transport limited. Similar mechanisms have been suggested for the slower growth rates of *Candidatus Nitrosacidococcus tergens* sp. RJ19 growing on urea as compared to ammonia (Picone et al. 2021). The longer acclimation period for comammox bacteria in urea-amended systems could also potentially be a reason for the lack of an association between comammox bacteria and NOB.

Altogether, our study demonstrates that comammox bacteria will dominate over canonical nitrifiers in communities sourced from nitrogen-limited environments irrespective of nitrogen source type or loading rate without directly competing with canonical AOB. Further, our study also indicates comammox bacteria and AOB may occupy independent niches in communities sources from low nitrogen environments. Interestingly, we see evidence of potential competitive exclusion of NOB by comammox bacteria governed by nitrogen source dependent metabolic coupling between AOB and NOB.

Funding

This work was supported by the NSF Graduate Research Fellowship (DGE-2019245309) and the Cochrane Fellowship to K.V. and by NSF-CBET Award number: 1703089.

Data availability

Raw sequence reads, metagenome assembly, and MAGs are available on NCBI at Bioproject number PRJNA764197.

Supplementary data

Supplementary data are available at [FEMSEC](#) online.

Acknowledgments

We thank anonymous reviewers for their thoughtful and constructive comments that helped improve this manuscript.

Conflict of interest statement. None declared.

References

Alneberg J, Bjarnason BS, de Bruijn I et al. Binning metagenomic contigs by coverage and composition. *Nat Methods* 2014; **11**:1144–6.

Annavajhala MK, Kapoor V, Santo-Domingo J et al. Comammox functionality identified in diverse engineered biological wastewater treatment systems. *Environ Sci Technol Lett* 2018; **5**:110–6.

Aramaki T, Blanc-Mathieu R, Endo H et al. KofamKOALA: KEGG ortholog assignment based on profile HMM and adaptive score threshold. *Bioinformatics* 2020; **36**:2251–2.

Bartelme RP, McLellan SL, Newton RJ. Freshwater recirculating aquaculture system operations drive biofilter bacterial community shifts around a stable nitrifying consortium of ammonia-oxidizing archaea and comammox nitrospira. *Front Microbiol* 2017; **8**:101.

Beach NK, Noguera DR. Design and assessment of species-level qPCR primers targeting comammox. *Front Microbiol* 2019; **10**:36.

Bollmann A, French E, Laanbroek HJ. Isolation, cultivation, and characterization of ammonia-oxidizing bacteria and archaea adapted to low ammonium concentrations. *Methods Enzymol* 2011; **486**: 55–88.

Bowers RM, Kyrpides NC, Stepanauskas R et al. Minimum information about a single amplified genome (MISAG) and a metagenome-assembled genome (MIMAG) of bacteria and archaea. *Nat Biotechnol* 2017; **35**:725–31.

Camejo PY, Santo Domingo J, McMahon KD et al. Genome-enabled insights into the ecophysiology of the comammox bacterium “*Candidatus nitrospira nitroosa*”. *Msystems* 2017; **2**:e00059–17.

Caporaso JG, Lauber CL, Walters WA et al. Global patterns of 16S rRNA diversity at a depth of millions of sequences per sample. *Proc Natl Acad Sci USA* 2011; **108 Suppl 1**:4516–22.

Chaumeil PA, Mussig AJ, Hugenholtz P et al. GTDB-Tk: a toolkit to classify genomes with the genome taxonomy database. *Bioinformatics* 2019; **36**:1925–27.

Chen S, Zhou Y, Chen Y et al. fastp: an ultra-fast all-in-one FASTQ preprocessor. *Bioinformatics* 2018; **34**:i884–90.

Cotto I, Dai Z, Huo L et al. Long solids retention times and attached growth phase favor prevalence of comammox bacteria in nitrogen removal systems. *Water Res* 2020; **169**:115268.

Daims H, Lebedeva EV, Pjevac P et al. Complete nitrification by Nitrospira bacteria. *Nature* 2015; **528**:504–9.

Daims H, Lucker S, Wagner M. A new perspective on microbes formerly known as nitrite-oxidizing bacteria. *Trends Microbiol* 2016; **24**:699–712.

Edgar RC. MUSCLE: a multiple sequence alignment method with reduced time and space complexity. *BMC Bioinf* 2004; **5**:113.

Eren AM, Esen OC, Quince C et al. Anvi'o: an advanced analysis and visualization platform for 'omics data. *PeerJ* 2015; **3**:e1319.

Fowler SJ, Palomo A, Dechesne A et al. Comammox Nitrospira are abundant ammonia oxidizers in diverse groundwater-fed rapid sand filter communities. *Environ Microbiol* 2018; **20**:1002–15.

Gonzalez-Martinez A, Rodriguez-Sanchez A, van Loosdrecht MCM et al. Detection of comammox bacteria in full-scale wastewater treatment bioreactors using tag-454-pyrosequencing. *Environ Sci Pollut Res Int* 2016; **23**:25501–11.

Gottshall EY, Bryson SJ, Cogert KI et al. Sustained nitrogen loss in a symbiotic association of Comammox Nitrospira and Anammox bacteria. *Water Res* 2020; **202**:117426.

Graham DW, Knapp CW, Van Vleck ES et al. Experimental demonstration of chaotic instability in biological nitrification. *ISME J* 2007; **1**:385–93.

Gruber-Vodicka HR, Seah BKB, Pruesse E. phyloFlash: rapid small-subunit rRNA profiling and targeted assembly from metagenomes. *mSystems* 2020; **5**:e00920–20.

Gulay A, Fowler SJ, Tatari K et al. DNA- and RNA-SIP reveal nitrospira spp. as key drivers of nitrification in groundwater-fed biofilters. *mBio* 2019; **10**:e01870–19.

Gulay A, Musovic S, Albrechtsen HJ et al. Ecological patterns, diversity and core taxa of microbial communities in groundwater-fed rapid gravity filters. *ISME J* 2016; **10**:2209–22.

Gurevich A, Saveliev V, Vyahhi N et al. QUAST: quality assessment tool for genome assemblies. *Bioinformatics* 2013; **29**:1072–5.

He S, Li Y, Mu H et al. Ammonium concentration determines differential growth of Comammox and canonical ammonia-oxidizing prokaryotes in soil microcosms. *Appl Soil Ecol* 2021; **157**:103776.

Hermannsson A, Lindgren PE. Quantification of ammonia-oxidizing bacteria in arable soil by real-time PCR. *Appl Environ Microbiol* 2001; **67**:972–6.

Hiroyuki Ogata SG, Sato K, Fujibuchi W et al. KEGG: kyoto encyclopedia of genes and genomes. *Nucleic Acids Res* 1999; **27**:27–30.

Hyatt D, Chen GL, Locascio PF et al. Prodigal: prokaryotic gene recognition and translation initiation site identification. *BMC Bioinf* 2010; **11**:119.

Jain C, Rodriguez RL, Phillippy AM et al. High throughput ANI analysis of 90K prokaryotic genomes reveals clear species boundaries. *Nat Commun* 2018;9:5114.

Kalyaanamoorthy S, Minh BQ, Wong TKF et al. ModelFinder: fast model selection for accurate phylogenetic estimates. *Nat Methods* 2017;14:587–9.

Kang DD, Li F, Kirton E et al. MetaBAT 2: an adaptive binning algorithm for robust and efficient genome reconstruction from metagenome assemblies. *PeerJ* 2019;7:e7359.

Kits KD, Sedlacek CJ, Lebedeva EV et al. Kinetic analysis of a complete nitrifier reveals an oligotrophic lifestyle. *Nature* 2017;549:269–72.

Koch H, Galushko A, Albertsen M et al. Growth of nitrite-oxidizing bacteria by aerobic hydrogen oxidation. *Science* 2014;345:1052–4.

Koch H, Lucker S, Albertsen M et al. Expanded metabolic versatility of ubiquitous nitrite-oxidizing bacteria from the genus *Nitrospira*. *Proc Natl Acad Sci USA* 2015;112:11371–6.

Koops H-P, Purkhold U, Pommerening-Röser A et al. The Lithoautotrophic Ammonia-Oxidizing Bacteria. In: Dworkin M, Falkow S, Rosenberg E et al. (eds). *The Prokaryotes*. New York: Springer, 2006, 778–811.

Kowalchuk GA, Stephen JR. Ammonia-oxidizing bacteria: a model for molecular microbial ecology. *Annu Rev Microbiol* 2001;55:485–529.

Letunic I, Bork P. Interactive tree of life (iTOL) v4: recent updates and new developments. *Nucleic Acids Res* 2019;47:W256–9.

Leung PM, Daebeler A, Chiri E et al. A nitrite-oxidizing bacterium constitutively consumes atmospheric hydrogen. *bioRxiv* 2021. DOI: 10.1101/2021.08.20.457082.

Li H, Durbin R. Fast and accurate short read alignment with burrows-wheeler transform. *Bioinformatics* 2009;25:1754–60.

Li H, Handsaker B, Wysoker A et al. The sequence alignment/map format and SAMtools. *Bioinformatics* 2009;25:2078–9.

Liu T, Wang Z, Wang S et al. Responses of ammonia-oxidizers and comammox to different long-term fertilization regimes in a subtropical paddy soil. *Eur J Soil Biol* 2019;93:103087.

Martens-Habbena W, Berube PM, Urakawa H et al. Ammonia oxidation kinetics determine niche separation of nitrifying Archaea and Bacteria. *Nature* 2009;461:976–9.

Menzel P, Ng KL, Krogh A. Fast and sensitive taxonomic classification for metagenomics with Kaiju. *Nat Commun* 2016;7:11257.

Na SI, Kim YO, Yoon SH et al. UBCG: up-to-date bacterial core gene set and pipeline for phylogenomic tree reconstruction. *J Microbiol* 2018;56:280–5.

Nguyen LT, Schmidt HA, von Haeseler A et al. IQ-TREE: a fast and effective stochastic algorithm for estimating maximum-likelihood phylogenies. *Mol Biol Evol* 2015;32:268–74.

Nurk S, Meleshko D, Korobeynikov A et al. metaSPAdes: a new versatile metagenomic assembler. *Genome Res* 2017;27:824–34.

Palatinszky M, Herbold C, Jehmlich N et al. Cyanate as an energy source for nitrifiers. *Nature* 2015;524:105–8.

Palomo A, Dechesne A, Smets BF. Genomic profiling of *Nitrospira* species reveals ecological success of comammox *Nitrospira*. *bioRxiv* 2019. DOI: 10.1101/612226.

Palomo A, Jane Fowler S, Gulay A et al. Metagenomic analysis of rapid gravity sand filter microbial communities suggests novel physiology of *Nitrospira* spp. *ISME J* 2016;10:2569–81.

Palomo A, Pedersen AG, Fowler SJ et al. Comparative genomics sheds light on niche differentiation and the evolutionary history of comammox *Nitrospira*. *ISME J* 2018;12:1779–93.

Parks DH, Imelfort M, Skennerton CT et al. CheckM: assessing the quality of microbial genomes recovered from isolates, single cells, and metagenomes. *Genome Res* 2015;25:1043–55.

Parks DH, Rinke C, Chuvochina M et al. Recovery of nearly 8000 metagenome-assembled genomes substantially expands the tree of life. *Nat Microbiol* 2017;2:1533–42.

Picone N, Pol A, Mesman R et al. Ammonia oxidation at pH 2.5 by a new gammaproteobacterial ammonia-oxidizing bacterium. *ISME J* 2021;15:1150–64.

Pinto AJ, Marcus DN, Ijaz UZ et al. Metagenomic evidence for the presence of comammox nitrospira-like bacteria in a drinking water system. *mSphere* 2016;1:e00054–15.

Pjevac P, Schauberger C, Poghosyan L et al. AmoA-targeted polymerase chain reaction primers for the specific detection and quantification of Comammox Nitrospira in the environment. *Front Microbiol* 2017;8:1508.

Poghosyan L, Koch H, Frank J et al. Metagenomic profiling of ammonia- and methane-oxidizing microorganisms in two sequential rapid sand filters. *Water Res* 2020;185:116288.

Poghosyan L, Koch H, Lavy A et al. Metagenomic recovery of two distinct Comammox Nitrospira from the terrestrial subsurface. *Environ Microbiol* 2019;21:3627–37.

Prosser JI, Nicol GW. Archaeal and bacterial ammonia-oxidisers in soil: the quest for niche specialisation and differentiation. *Trends Microbiol* 2012;20:523–31.

Pruesse E, Quast C, Knittel K et al. SILVA: a comprehensive online resource for quality checked and aligned ribosomal RNA sequence data compatible with ARB. *Nucleic Acids Res* 2007;35:7188–96.

Quinlan AR, Hall IM. BEDTools: a flexible suite of utilities for comparing genomic features. *Bioinformatics* 2010;26:841–2.

Rognes T, Flouri T, Nichols B et al. VSEARCH: a versatile open source tool for metagenomics. *PeerJ* 2016;4:e2584.

Roots P, Wang Y, Rosenthal AF et al. Comammox Nitrospira are the dominant ammonia oxidizers in a mainstream low dissolved oxygen nitrification reactor. *Water Res* 2019;157:396–405.

Sakoula D, Koch H, Frank J et al. Enrichment and physiological characterization of a novel comammox Nitrospira indicates ammonium inhibition of complete nitrification. *ISME J* 2020;15:1010–24.

Sedlacek CJ, McGowan B, Suwa Y et al. A physiological and genomic comparison of nitrosomonas cluster 6a and 7 ammonia-oxidizing bacteria. *Microb Ecol* 2019;78:985–94.

Seemann T. Prokka: rapid prokaryotic genome annotation. *Bioinformatics* 2014;30:2068–9.

Shao YH, Wu JH. Comammox nitrospira species dominate in an efficient partial nitrification-anammox bioreactor for treating ammonium at low loadings. *Environ Sci Technol* 2021;55:2087–98.

Shi X, Hu H-W, Wang J et al. Niche separation of Comammox Nitrospira and canonical ammonia oxidizers in an acidic subtropical forest soil under long-term nitrogen deposition. *Soil Biol Biochem* 2018;126:114–22.

Sieber CMK, Probst AJ, Sharrar A et al. Recovery of genomes from metagenomes via a dereplication, aggregation and scoring strategy. *Nat Microbiol* 2018;3:836–43.

Spasov E, Tsuji JM, Hug LA et al. High functional diversity among *Nitrospira* populations that dominate rotating biological contactor microbial communities in a municipal wastewater treatment plant. *ISME J* 2020;14:1857–72.

Stahl DA, de la Torre JR. Physiology and diversity of ammonia-oxidizing archaea. *Annu Rev Microbiol* 2012;66:83–101.

Tatari K, Musovic S, Gulay A et al. Density and distribution of nitrifying guilds in rapid sand filters for drinking water production: dominance of *Nitrospira* spp. *Water Res* 2017;127:239–48.

van Kessel MA, Speth DR, Albertsen M et al. Complete nitrification by a single microorganism. *Nature* 2015;528:555–9.

Wang J, Wang J, Rhodes G et al. Adaptive responses of Comammox Nitrospira and canonical ammonia oxidizers to long-term fer-

tilizations: implications for the relative contributions of different ammonia oxidizers to soil nitrogen cycling. *Sci Total Environ* 2019a;**668**:224–33.

Wang M, Huang G, Zhao Z et al. Newly designed primer pair revealed dominant and diverse Comammox amoA gene in full-scale wastewater treatment plants. *Bioresour Technol* 2018;**270**:580–7.

Wang X, Wang S, Jiang Y et al. Comammox bacterial abundance, activity, and contribution in agricultural rhizosphere soils. *Sci Total Environ* 2020;**727**:138563.

Wang Y, Ma L, Mao Y et al. Comammox in drinking water systems. *Water Res* 2017;**116**:332–41.

Wang Z, Cao Y, Zhu-Barker X et al. Comammox Nitrospira clade B contributes to nitrification in soil. *Soil Biol Biochem* 2019b;**135**:392–5.

Wu YW, Simmons BA, Singer SW. MaxBin 2.0: an automated binning algorithm to recover genomes from multiple metagenomic datasets. *Bioinformatics* 2016;**32**:605–7.

Xu S, Chai W, Xiao R et al. Survival strategy of comammox bacteria in a wastewater nutrient removal system with sludge fermentation liquid as additional carbon source. *Sci Total Environ* 2022;**802**:149862.

Yang Y, Daims H, Liu Y et al. Activity and metabolic versatility of complete ammonia oxidizers in full-scale wastewater treatment systems. *Mbio* 2020;**11**:e03175–19.

Zheng M, Wang M, Zhao Z et al. Transcriptional activity and diversity of comammox bacteria as a previously overlooked ammonia oxidizing prokaryote in full-scale wastewater treatment plants. *Sci Total Environ* 2019;**656**:717–22.